

FULL-LENGTH ORIGINAL RESEARCH

Focal generation of paroxysmal fast runs during electrographic seizures

*Sofiane Boucetta, *Sylvain Chauvette, †Maxim Bazhenov, and *Igor Timofeev

*Department of Anatomy and Physiology Laval University, Quebec, Canada; and †The Salk Institute, Computational Neurobiology Laboratory, La Jolla, California, U.S.A.

SUMMARY

Purpose: A cortically generated Lennox-Gastaut type seizure is associated with spike-wave/poly-spike-wave discharges at 1.0–2.5 Hz and fast runs at 7–16 Hz. Here we studied the patterns of synchronization during runs of paroxysmal fast spikes.

Methods: Electrographic activities were recorded using multisite intracellular and field potential recordings *in vivo* from cats anesthetized with ketamine-xylazine. In different experiments, the recording electrodes were located either at short distances (<1 mm) or at longer distances (up to 12 mm). The main experimental findings were tested in computational models.

Results: In the majority of cases, the onset and the offset of fast runs occurred almost simultaneously in different recording sites. The amplitude and duration of fast runs could vary by orders of magnitude. Within the fast runs, the patterns of synchronization recorded in different electrodes

were as following: (1) synchronous, in phase, (2) synchronous, with phase shift, (3) patchy, repeated in phase/phase shift transitions, and (4) nonsynchronous, slightly different frequencies in different recording sites or absence of oscillatory activity in one of the recording sites; the synchronous patterns (in phase or with phase shifts) were most common. All these patterns could be recorded in the same pair of electrodes during different seizures, and they were reproduced in a computational network model. Intrinsically bursting (IB) neurons fired more spikes per cycle than any other neurons suggesting their leading role in the fast run generation.

Conclusions: Once started, the fast runs are generated locally with variable correlations between neighboring cortical foci.

KEY WORDS: Synchronization, Cortex, Electrographic seizures, Intracellular, *In vivo*, Computational model.

Sleep-related epilepsy is characterized by seizures developing during periods of slow-wave sleep. Studies on experimental animals point to the intracortical origin of some specific types of such seizures (Steriade & Contreras, 1998). These seizures are characterized by spike-wave (SW) or spike-wave/polyspike-wave (SW/PSW) complexes of 1–2.5 Hz, intermingled with episodes of fast runs at ~7–16 Hz (Neckelmann et al., 1998; Steriade & Contreras, 1998; Steriade et al., 1998a; Timofeev et al., 1998). The evolution of these seizures from the corti-

cally generated slow oscillation may be shaped by the thalamus (Steriade & Contreras, 1995; Steriade et al., 1998a; Steriade & Timofeev, 2001; Hughes et al., 2002; Meeren et al., 2002). The electrographical pattern of these seizures as well as their occurrence during slow-wave sleep resembles the seizures accompanying Lennox-Gastaut syndrome of humans (Halasz, 1991; Kotagal, 1995; Niedermeyer, 2005a; Niedermeyer, 2005b). The prolonged (more than 2–3 s) periods of runs of fast electroencephalography (EEG) spikes were usually associated with tonic components of seizures accompanying Lennox-Gastaut syndrome (Niedermeyer, 2005a). Less frequently, fast runs occur in other epileptic conditions (Niedermeyer, 2005a). The detailed pattern of synchronization as well as the cellular basis of fast runs is not well understood. Previous single-case human study has shown that an increase in the synchronization stops the runs of fast EEG spikes (Ferri et al.,

Accepted May 7, 2008; Online Early publication xxxxxx xx
xxxx.

Address correspondence to Igor Timofeev, Department of Anatomy and Physiology Laval University, Quebec, Canada. E-mail: Igor.Timofeev@phs.ulaval.ca

Wiley Periodicals, Inc.

© 2008 International League Against Epilepsy

2004). Animal studies showed that (1) the thalamus is not involved in the generation of fast runs (Timofeev et al., 1998), (2) the inhibitory activities in neocortex are impaired during the fast runs (Timofeev et al., 2002), and (3) these changes occur in parallel with a decrease in the neuronal input resistance (Matsumoto et al., 1969; Neckelmann et al., 2000; Timofeev et al., 2002) and a decrease in the concentration of extracellular calcium (Heinemann et al., 1977; Amzica et al., 2002).

During normal (not paroxysmal) brain activities, both the excitatory and inhibitory synaptic interactions provide mechanisms for the synchronization among neighboring recording sites. In a condition of low extracellular Ca^{2+} concentration (decrease in synaptic interactions), impaired inhibitory activities, and low input resistance, as observed during seizures (see above), the synchrony should be reduced. Thus, we hypothesize that paroxysmal runs of fast EEG spikes are generated more locally (compare with normal electrophysiological activities) with minimal, if any, involvement of long-range connections; neighboring foci oscillate in a quasi-independent manner. The present study supports this hypothesis and provides data on the neuronal basis and patterns of synchronization during fast runs generated within spontaneous electrographic seizures. The present study also contains a network model that reproduces the main patterns of synchronization encountered with *in vivo* recordings and that supports the presented hypothesis.

MATERIALS AND METHODS

In vivo experiments

Experiments were conducted on adult cats anesthetized with ketamine-xylazine anesthesia [10–15 and 2–3 mg/kg intramuscular (i.m.), respectively]. The animals were paralyzed with gallamine triethiodide (20 mg/kg) after the EEG showed typical signs of deep general anesthesia, essentially consisting of a slow oscillation (0.5–1 Hz). Supplementary doses of the same anesthetics (5 and 1 mg/kg) or simply ketamine (5 mg/kg) were administered at the slightest changes toward the diminished amplitudes of slow waves. The cats were ventilated artificially with the control of end-tidal CO_2 at 3.5%–3.7%. The body temperature was maintained at 37°–38°C, and the heart rate was ~90–100 beats/min. For intracellular recordings, the stability was ensured by the drainage of cisterna magna, hip suspension, bilateral pneumothorax, and by filling the hole made for recordings with a solution of 4% agar. At the end of experiments, the cats were given a lethal dose of pentobarbital [50 mg/kg intravenous (i.v.)]. All experimental procedures were performed according to the National Institutes of Health (NIH) and national guidelines and were approved by the committee for animal care of Laval University.

Single, dual, triple, or quadruple intracellular recordings from suprasylvian associative areas 5 and 7 were performed using glass micropipettes filled with a solution of 3 M potassium-acetate (KAc). A high-impedance amplifier with active bridge circuitry was used to record the membrane potential (V_m) and inject current into the neurons. Field potentials were recorded in the vicinity of impaled neurons and also from more distant sites, using bipolar coaxial electrodes, with the ring (pial surface) and the tip (cortical depth) separated by 0.8–1 mm. In 12 cats, arrays of 7 or 8 low impedance tungsten electrodes, ~1.5 mm apart, were inserted along the suprasylvian gyrus. All electrical signals were sampled at 20 kHz and digitally stored on Vision (Nicolet Instrument Technologies, Madison, WI, U.S.A.). Offline computer analysis of electrographic recordings was done with IgorPro software (WaveMetrics, Lake Oswego, OR, U.S.A.). Statistical analysis was conducted with JMP software (SAS Institute, Cary, NC, U.S.A.). All numerical values are expressed as a mean \pm standard deviation.

Computational model

A cortical model consisting in a one-dimensional chain of 100 pyramidal (PY) neurons and 25 interneurons (INs) was simulated. The connection fan out was ± 5 neurons for α -amino-3-hydroxy-5-methyl-4-isoxazole-propionic acid (AMPA) mediated PY-PY synapses, ± 1 neuron for AMPA-mediated PY-IN synapses, and ± 5 neurons for GABA_A-mediated IN-PY synapses. All AMPA- and GABA_A-mediated synapses were modeled by first-order activation schemes (Destexhe et al., 1994), and the expressions for the kinetics are given elsewhere (Bazhenov et al., 1998). A simple model of synaptic plasticity was used to describe depression of synaptic connections (Abbott et al., 1997; Tsodyks & Markram, 1997; Bazhenov et al., 1998; Galarreta & Hestrin, 1998; Timofeev et al., 2000). A maximal synaptic conductance was multiplied to depression variable, $D \leq 1$, representing the amount of available “synaptic resources”: $D = 1 - (1 - D_i(1-U)) \exp(-(t-t_i)/\tau)$, where $U = 0.07$ is the fraction of resources used per action potential, $\tau = 700$ ms the time constant of recovery of the synaptic resources, D_i the value of D immediately before the i_{th} event, and $(t-t_i)$ the time after i_{th} event.

Each PY and IN cell was modeled by two compartments that included fast Na^+ channels, I_{Na} , and a persistent sodium current, $I_{\text{Na(p)}}$ (Alzheimer et al., 1993; Kay et al., 1998), in the axosomatic and the dendritic compartments (Mainen & Sejnowski, 1996). A slow voltage-dependent noninactivating K^+ current, $I_{\text{K(m)}}$, a slow Ca^{2+} dependent K^+ current, $I_{\text{K(Ca)}}$, a high-threshold Ca^{2+} current, I_{Ca} , hyperpolarization-activated depolarizing current, I_{h} , were included in the dendritic compartment. A fast delayed rectifier potassium K^+ current, I_{K} , was present in the axosomatic compartment. The expressions for the voltage- and Ca^{2+} -dependent transition rates for all other

currents are given in (Bazhenov et al., 2002; Frohlich & Bazhenov, 2006). Reversal potentials for all K^+ -mediated currents were calculated using Nernst equation. The extracellular K^+ concentration was continuously updated based on K^+ currents, K^+ pumps, and K^+ buffering simulating the glial K^+ uptake system (Bazhenov et al., 2004). The glial buffering was modeled by first-order kinetics (Kager et al., 2000). The firing properties of this two-compartmental model depend on the coupling conductance between compartments ($g = 1/R$, where R is resistance between compartments), and the ratio of dendritic area to axosomatic area. The ratio, r , controls the firing patterns in the model (Mainen & Sejnowski, 1996). We used a model of a regular-spiking neuron for PY cells ($r = 165$) and a model of a fast-spiking neuron for IN cells ($r = 50$). The firing patterns of these cell types in response to direct current (DC) pulses of different amplitude are shown in our previous publication (see Fig. 3B in Rulkov et al., 2004).

RESULTS

In vivo experiments

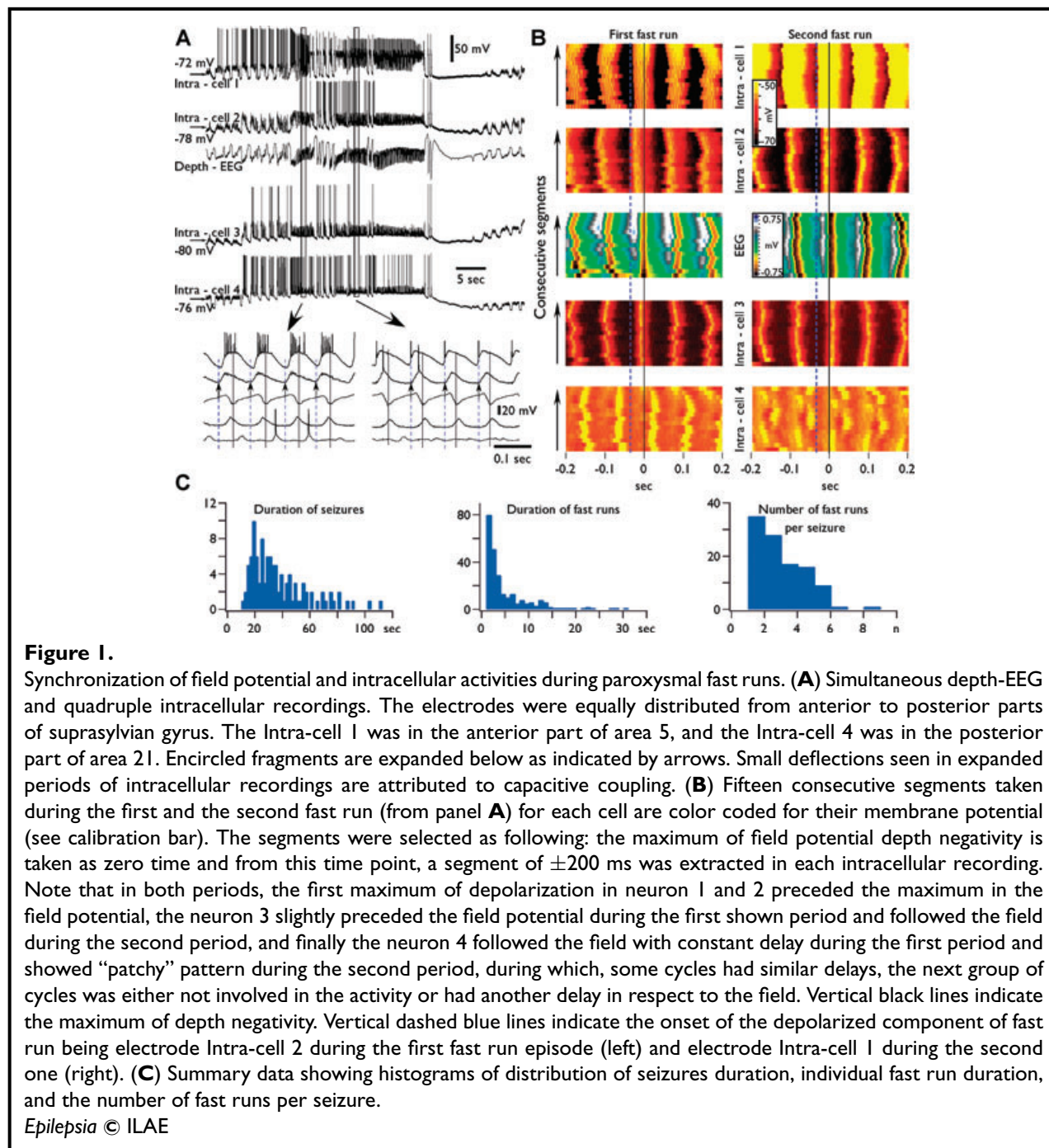
Experimental model and database

We performed various experiments to study different aspects of thalamocortical physiology between the years 2001 and 2006. During these experiments, some of the cats displayed electrographic seizures. In these animals, we stopped the initially thought experiment and changed experimental approach to address the hypothesis described in the introduction of the present study. We recorded electrophysiological activities from 87 cats initially anesthetized with ketamine-xylazine. Typically, supplementary doses of anesthesia were administered every hour. In 41 cats, an initial anesthesia was followed by additional doses of ketamine. Similar to other studies (Steriade & Contreras, 1995), in these experiments, ~30% of cats (12 cats out of 41) developed spontaneous paroxysmal discharges. Adding ketamine-xylazine as supplementary anesthetic resulted in the generation of electrographic seizures in ~75% of cats (35 out of 46). Usually, the seizures started after administration of the third-fourth supplementary dose. These seizures, consisting of SW complexes at 1–2.5 Hz or SW/PSW complexes associated with fast runs at 7–16 Hz, were developed from sleep-like slow rhythm. As in our previous study (Grenier et al., 2003b), the seizures were preceded by ripples, or the onset of seizures occurred simultaneously with them in at least one recording electrode (not shown). In total, we analyzed 224 electrographic seizures recorded with field potential electrodes. In parallel with EEG recording, we recorded intracellular activities of 157 neurons. This includes 8 simultaneous quadruple, 15 triple, and 22 dual records. In 11 neurons, we recorded more than 20 seizures.

An example of typical seizure is shown in Fig. 1A, in which the first 5 s show a normal slow oscillation. The beginning of electrographic seizure was associated with amplifier EEG waves and amplifier intracellularly recorded depolarizing potentials repeated at frequencies 1.0–2.5 Hz. Examples of transition from slow oscillation to seizures at larger scale could be found in our previous publications (Figs. 1 and 2 in Timofeev et al., 1998; Fig. 10 in Timofeev et al., 2002; and Fig. 8 in Frohlich et al., 2006). In some neurons, the enhanced depolarizing potentials were associated with an increased firing (as in neuron 1 and neuron 4 in Fig. 1). After several cycles of SW/PSW discharges the activity switched to runs of paroxysmal spikes (7–16 Hz) during which the long-lasting depth-positive EEG waves and associated intracellular hyperpolarizing potentials were absent. The fast runs appeared as a prolongation of PSW complexes. In this study, the polyspike discharges exceeding 1 s were considered as runs of fast EEG spikes. The total duration of seizures was between 10 and 120 s (37.2 ± 22.2 s, mean \pm SD, Fig. 1C). We analyzed 252 periods of fast runs, which lasted between 1 and 30 s (4.9 ± 5.7 s, Fig. 1C). Out of these, 174 periods lasted for less than 5 s. Each electrographic seizure recorded in these experimental conditions could have several periods of fast runs (1–8, mean 2.4 ± 1.4 , Fig. 1C) and SW complexes. Below, we will focus on the generation of paroxysmal runs of fast spikes.

Multisite distant recordings during fast runs

Using multisite recordings, we evaluated the patterns of synchronization between field potentials and intracellular activities during fast runs. Within the fast runs, the patterns of synchronization recorded with different electrodes were as following: (1) synchronous, in phase, (2) synchronous, with phase shift (one recording preceded or followed the activity in reference electrode), (3) “patchy,” repeated in phase/phase shift transitions, and (4) nonsynchronous, different frequencies in different recording sites or absence of rhythmic activities at one of the recording sites (see Fig. 4C). All these patterns could be recorded in the same pair of electrodes during different seizures. Generally, the frequency of activity during the same period of relatively short (<5 s) fast runs remained similar in different recording sites, but the phase-shifts were very variable during different epochs of the fast runs. Some of these patterns are illustrated in Fig. 1, where a field potential recording and a quadruple intracellular recording were used. In this experiment, the electrodes were located in the suprasylvian gyrus: Intra-cell 1 was located in the anterior part of area 5, the other electrodes were equally spaced with a distance between neighboring electrodes of about 4 mm in the posterior direction. The seizure contained three periods of fast runs (two of them are shown at a higher time resolution in the Fig. 1, A and B). During the first period of fast runs, the maximal depolarization of neurons 1, 2, and 3 preceded



the maximal field potential depth-negativity and the maximal depolarization of neuron 4 followed the field potential (see black lines in Fig. 1, A and B). The onset of each oscillatory cycle occurred first at the electrode Intra-cell 2 (see blue dotted lines in Fig. 1) during all the cycles of this period of fast runs (Fig. 1B). During the second period of fast runs, Intra-cell 1 was always the first in the generation of each oscillatory cycle. The onset of depolarization in neuron 2, occurred coincidentally with the spike in the neuron 1; the onset of depolarization in the neuron 3 was

delayed, and the delay fluctuated in 20–30 ms range. The oscillatory activity in the neuron 4 was damped, and the neuron 4 revealed a patchy pattern of activity; there was a phase shift during each several cycles (Fig. 1B). Thus, the multisite intracellular and field potential recordings revealed that runs of fast spikes behave as quasi-independent oscillators (see also Derchansky et al., 2006).

To characterize the patterns of synchronization during fast runs, we performed cross-correlation analysis. As expected, during the SW/PSW complexes, the

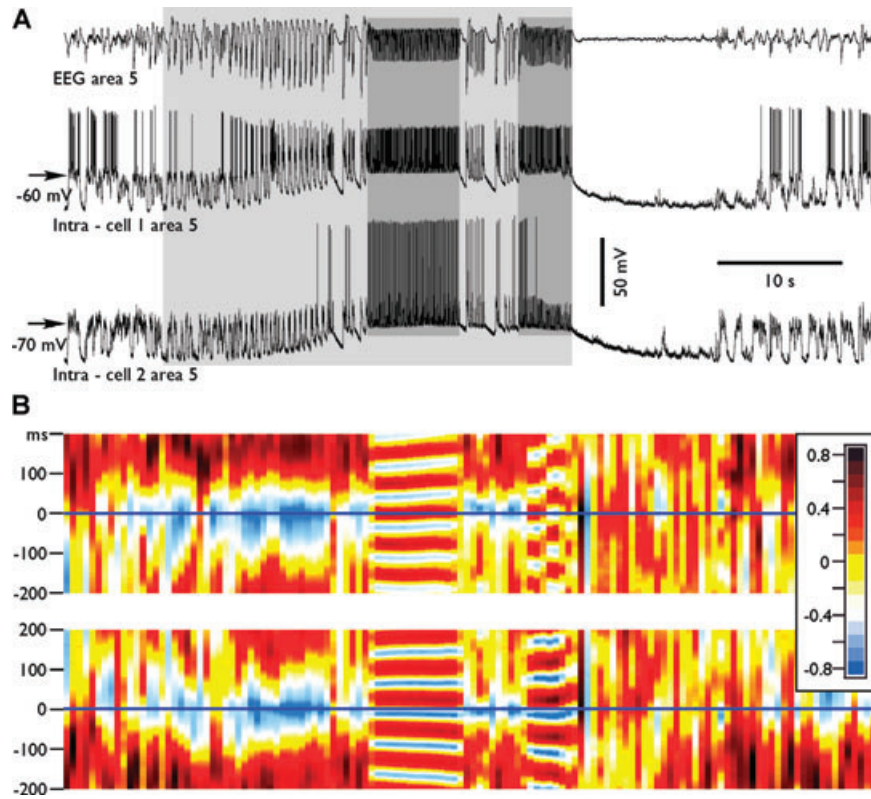


Figure 2.

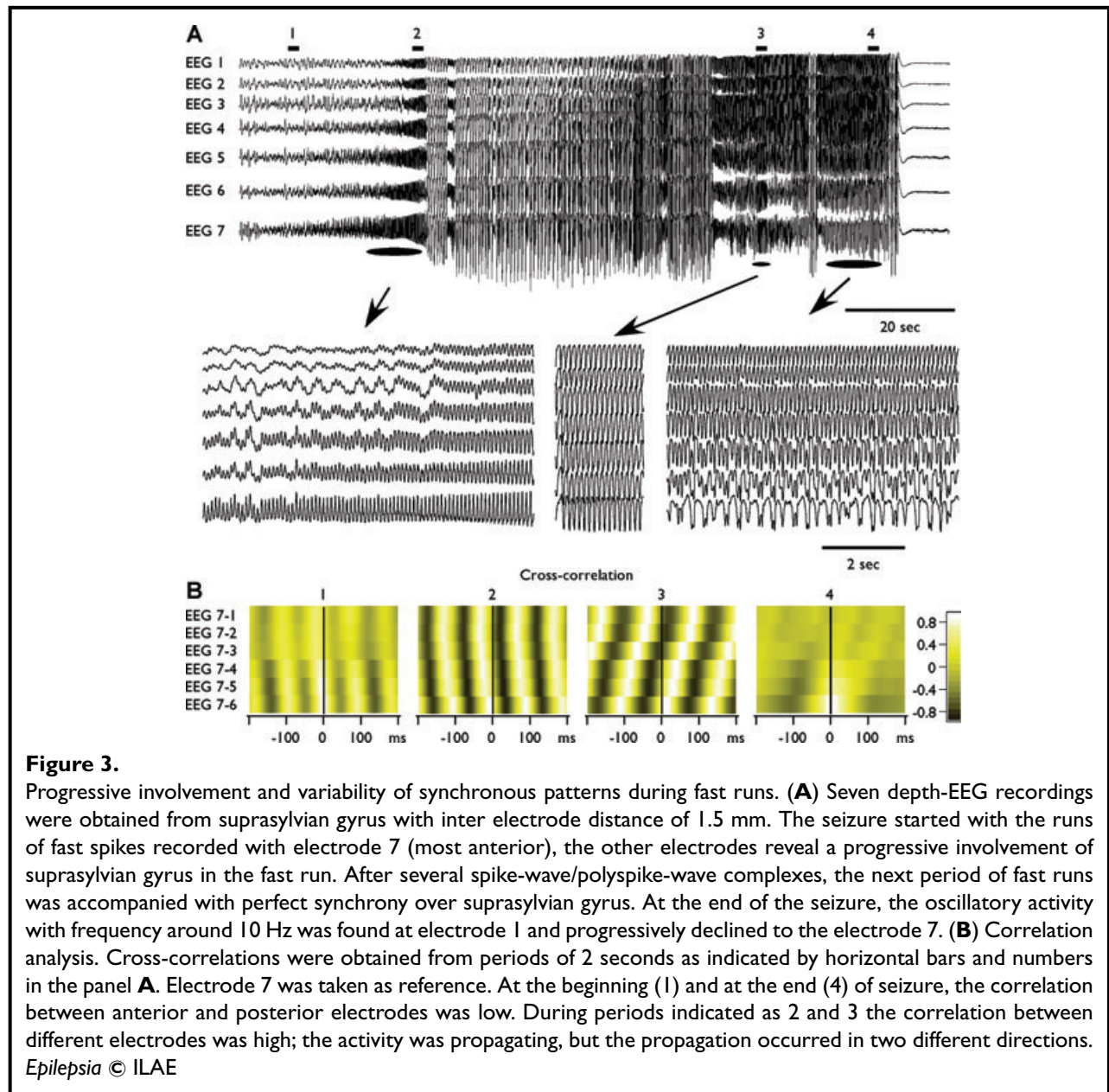
Dynamics of cross-correlation during paroxysmal fast runs. **(A)** Depth-EEG and dual intracellular recordings during a seizure containing two periods of fast runs. **(B)** The consecutive cross-correlations between EEG and neurons. The running correlogram was calculated as following: for a time interval of 1.0 s, the correlation function between two channels was calculated with correlation length ± 0.2 s. Frame was then moved with a step of 0.5 s, correlation calculated, color-coded, plotted, and so on. Each of correlated periods is represented as a single color strip in the bottom panels. Note that during spike-wave discharges the correlation between neuron and EEG was negative, as expected. During the first period of fast runs, the neuron 1 had reversed phase relations with EEG, while during the second period of fast runs, the neuron revealed a patchy pattern. It oscillated several cycles in phase and another several cycles in counter phase; the neuron 2 oscillated in phase with the EEG during both spike-wave complexes and during both periods of fast runs.

Epilepsia © ILAE

cross-correlation between intracellular activities and EEG was generally negative since active periods were characterized by neuronal depolarization and depth-negative EEG waves, and during depth-positive EEG waves the neurons were hyperpolarized (Fig. 2). The fast runs were characterized by variable patterns of synchronization. In the majority of cases (70%), the delay between the two recording leads was stable throughout the period of fast runs. As shown in the example in Fig. 2B, the Intra-cell 1 preceded the EEG by about 35 ms during the first period of fast runs. However, during the second period of fast runs, the intracellular activities of this neuron preceded the EEG during the first half, and it was synchronous in phase oscillation during the second half of the same period of fast runs. The second neuron (Intra-cell 2) and EEG had stable re-

lation during fast runs, and the maximum of neuronal excitation preceded the EEG with delay of about 10 ms during both periods of fast runs (Fig. 2B). Therefore the neuron 1 revealed patchy pattern suggesting that fast runs are generated with very limited, in any, communication between cortical foci.

Although in the vast majority of cases the periods of fast runs occurred almost simultaneously in all recording leads along the suprasylvian gyrus, on some occasions, the pattern was different. The Fig. 3 shows an example in which the seizure started from the fast run generated in the anterior part of suprasylvian cortex (EEG 7). The correlation between anterior and posterior electrodes had small values (Fig. 3B, 1). Progressively, this activity involved more posterior regions of suprasylvian gyrus, and the oscillation

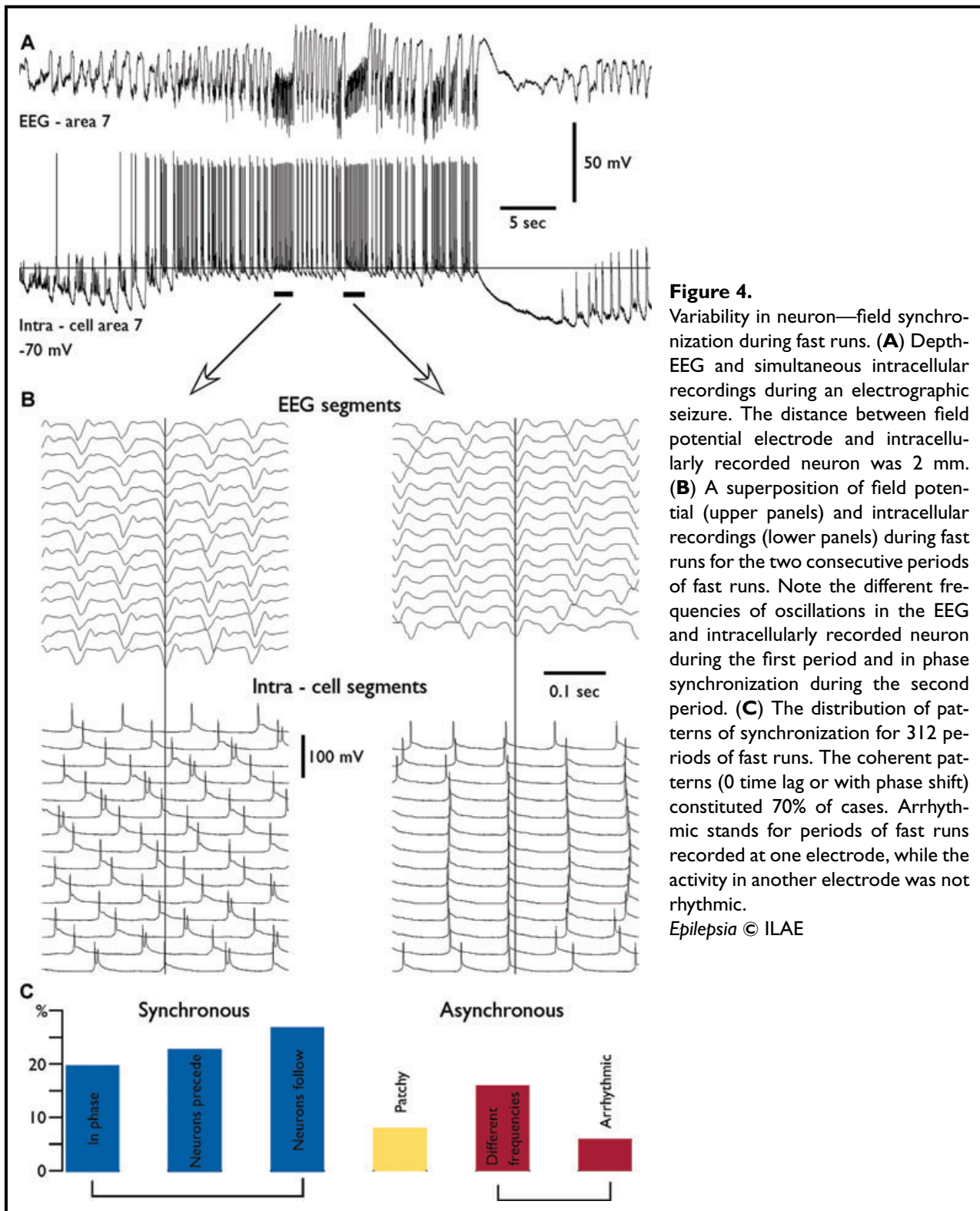


with a frequency of 11 Hz becomes dominant on all 7 EEG leads with a high value of correlation accompanied by a rapid propagation of activity in posterior-anterior direction (Fig. 3B, 2). Another period of the fast runs, during the same seizure, started almost simultaneously in all EEG electrodes (frequency 8.5 Hz, see the middle expanded part in Fig. 3A), and the correlation between all electrodes was high with a marked anterior-posterior propagation (Fig. 3B, 3). At the end of the seizure, the fast runs (9.5 Hz) were dominant in the posterior part of suprasylvian gyrus, while the anterior suprasylvian gyrus displayed frequency around 4 Hz, therefore the anterior-posterior correlation was low (Fig. 3B, 4).

Thus, our multisite recordings (both intra- and extracellular) demonstrated that in the majority of cases the onset and the end of runs of fast spikes occurred almost simultaneously at different locations. However, either the frequency of oscillation or the phase shifts between different locations were dissimilar in each period of fast runs. The dominating pattern of activity could switch even during the same epoch of fast runs.

Divergence of synchronizing patterns during fast runs

The phase shift during the same run of fast spikes could be very variable when it is recorded with two or more electrodes located at distances larger than several millimeters

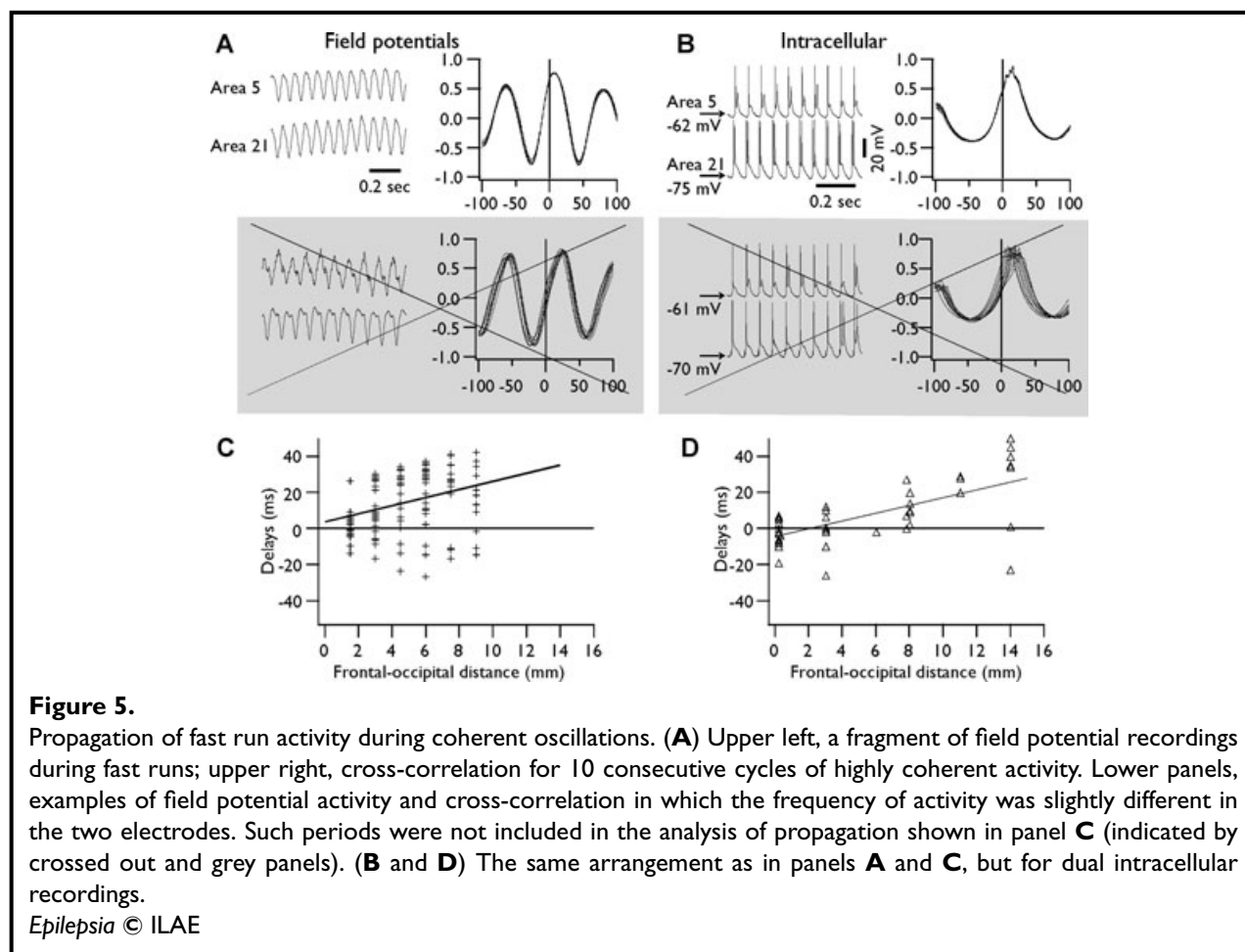
**Figure 4.**

Variability in neuron—field synchronization during fast runs. **(A)** Depth-EEG and simultaneous intracellular recordings during an electrographic seizure. The distance between field potential electrode and intracellularly recorded neuron was 2 mm. **(B)** A superposition of field potential (upper panels) and intracellular recordings (lower panels) during fast runs for the two consecutive periods of fast runs. Note the different frequencies of oscillations in the EEG and intracellularly recorded neuron during the first period and in phase synchronization during the second period. **(C)** The distribution of patterns of synchronization for 312 periods of fast runs. The coherent patterns (0 time lag or with phase shift) constituted 70% of cases. Arrhythmic stands for periods of fast runs recorded at one electrode, while the activity in another electrode was not rhythmic.

Epilepsia © ILAE

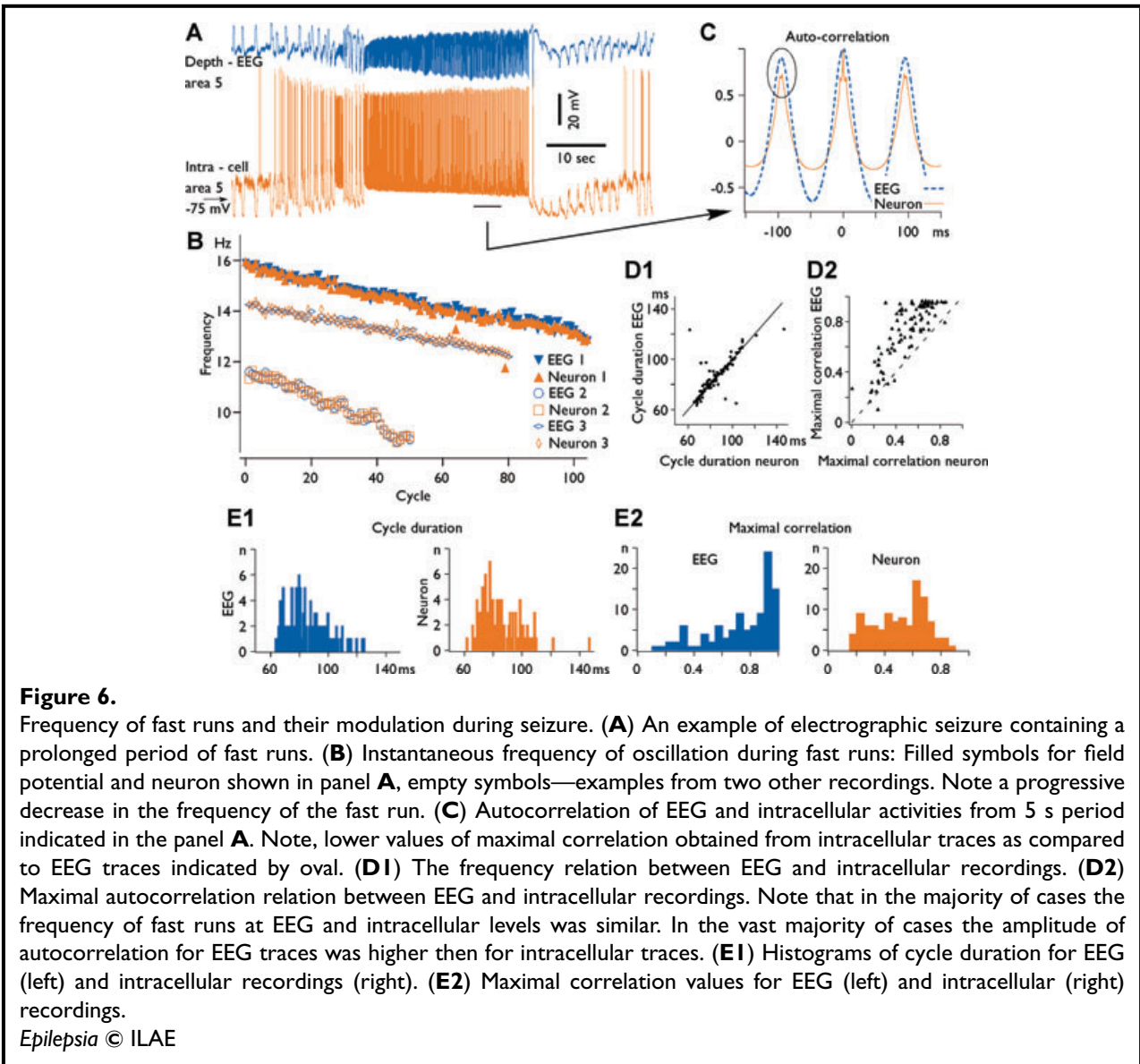
(Figs. 1–3). In long-lasting recordings (longer than 10 min), we analyzed the patterns of synchronization during fast runs between neurons and field potential recorded at about 1 mm apart (Fig. 4). We found that each pair

of records (cell-EEG) had a preferred phase relationship, but on some occasions, it revealed significant variations in the pattern of synchronization. Even in close recordings the pattern of synchronization during fast runs could vary



within the same seizure. During one period of fast runs, the oscillation in two electrodes could be synchronous, while during another period it could be of different frequencies (Fig. 4). As an extreme case, we recorded large amplitude EEG fast runs and absence of such or similar oscillation in a closely located neuron ($n = 5$), while the previous or the following periods of fast runs showed synchronous oscillations in both electrodes (not shown). We analyzed the pattern of synchronization between activities recorded with intracellular and nearby field potential electrodes during 312 periods of fast runs (Fig. 4C). We found that in only 20% of cases the oscillation was in phase (the neuron fired around maximum of the EEG depth-negative wave). However, the phase-locked patterns of activity (with or without different delays) were recorded in 70% of cases. In 22% of cases, the activity was not synchronous; either two sites revealed oscillation with different frequencies or the recording revealed arrhythmic activity (Fig. 4C). In 8% of cases, the activity was patchy; there were two or more changes in the pattern of synchronization during the same period of fast run (see examples in Fig. 1, Intra-cell 4, second period, and Fig. 2 Intra-cell 1, second period).

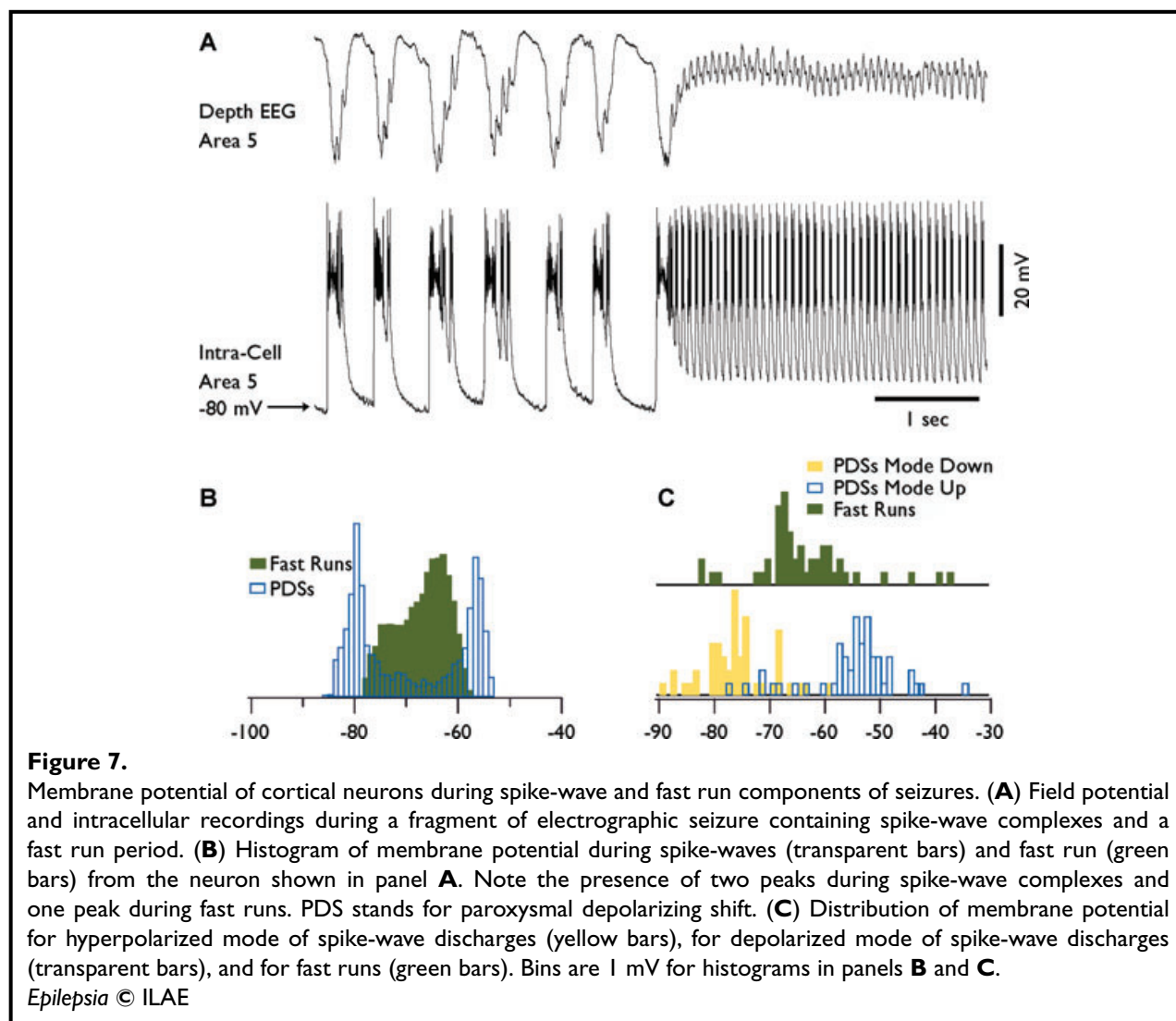
We systematically analyzed the spatial synchronization of fast runs within suprasylvian gyrus of cats. For this analysis, we have chosen only periods of fast runs that revealed consistent delays of coherent activity over 10 or more consecutive cycles with variability of cross-correlation maximums not exceeding 2 ms (Fig. 5). We analyzed separately pairs of EEG recordings and pairs of intracellular recordings obtained at different distances. In most of the cases, the activity in the more anterior electrodes preceded the activity in the more posterior electrodes. We found that the fast run activity could propagate with a maximal velocity reaching 10 m/s; however, the mean velocity was estimated as 2.13 ± 0.38 m/s from pairs of EEG electrodes and 2.23 ± 0.60 m/s from pairs of cells, indicating the presence of similar delays detected with two different methods of recordings. During consecutive fast runs, the same pair of either EEG or intracellular recordings could reveal propagation from -5 m/s (posterior to anterior) to 8 m/s (anterior to posterior). Thus, each period of fast runs was characterized by unique propagation velocity and direction of propagation. However, the recordings from closely located neurons (<0.2 mm lateral distance) revealed that the coherent



oscillation between two neurons could be delayed by up to 20 ms, which corresponds to very slow propagation speed of <10 mm/s. This suggests that these two cells were oscillating in an independent manner. Thus, similar to studies in disinhibited slices, if propagation of activity takes place, its velocity varied manyfold (Chervin et al., 1988).

In a sample of 115 periods of fast runs that lasted 5 s or longer we analyzed the duration of oscillatory cycles (Fig. 6). The frequency of oscillation during the prolonged periods (>10 s) of fast runs usually underwent a progressive decrease (Fig. 6B). To estimate the duration of a cycle during different periods of the same fast run, we obtained autocorrelations for consecutive periods lasting 5 s (Fig. 6C). At the beginning of the prolonged fast runs the mean frequency of oscillation was 13.8 ± 2.0 Hz and at the end, it was slightly but significantly slower 11.3 ± 2.1

Hz (paired Student's *t*-test, $p = 0.007$). The decrease in frequency on cycle-by-cycle basis was 0.036 ± 0.016 Hz. The duration of cycles for neurons and EEG was usually similar and varied from 62 ms to 124 ms (16 Hz to 8 Hz, Fig. 6, D1 and E1). However, during some period of fast runs the difference could be as large as a double of the frequency. We calculated rhythm coefficient, measured as the amplitude of the second peak of autocorrelation, being 1 when all cycles had identical frequency and 0 when all cycles had different frequency. The rhythm coefficient obtained from the field potential recordings during fast runs was very high, and for 75% of cases it was above 0.8, suggesting a high periodicity of cycles (Fig. 6E, 2). The intracellular traces revealed slightly lower values of correlation (Fig. 6, D2 and E2). This was likely because the variability of cycle duration for one neuron was larger than for field potential



recordings; field potentials reflect the averaged activity of a set of neurons and glial cells and thus, they are much less sensitive to the variability in individual cycles of individual cells.

Membrane potential during fast runs

The membrane potential during SW components of seizures had a bimodal distribution and exposed two relatively stable states. In the recording shown in (Fig. 7A) the neuron was hyperpolarized to -80 mV during EEG wave component, and it was depolarized to -55 mV during EEG spike component as revealed by the histogram of membrane potential distribution (Fig. 7B). During fast runs, the membrane potential oscillated continuously, and only one peak could be detected from the histogram of membrane potential distribution, which was in between the peak values of membrane potential during depolarized and hyperpolarized states (Fig. 7B). To quantify the peak values of membrane potential in a population of neurons we used

the modal values for depolarized and hyperpolarized states and fast runs. The histograms of membrane potential distribution for 50 neurons demonstrate that the majority of neurons had their modal membrane potential values during fast runs between that of depolarized and hyperpolarized states during SW complexes (Fig. 7C). The membrane potential during fast runs was by 9.11 ± 1.13 mV ($p < 0.0001$) more hyperpolarized than during the depolarized components of SW discharges. There were significant correlations ($r = 0.57$, $p < 0.0001$) between the membrane potential during fast runs and depolarizing component of seizures.

Intrinsic neuronal properties and fast runs

All neurons that were recorded during both, electrographic seizures and periods outside seizures ($n = 157$), were classified by electrophysiological criteria as regular-spiking (RS), fast-rhythmic-bursting (FRB), intrinsically-bursting (IB), and fast-spiking (FS) (Connors & Gutnick,

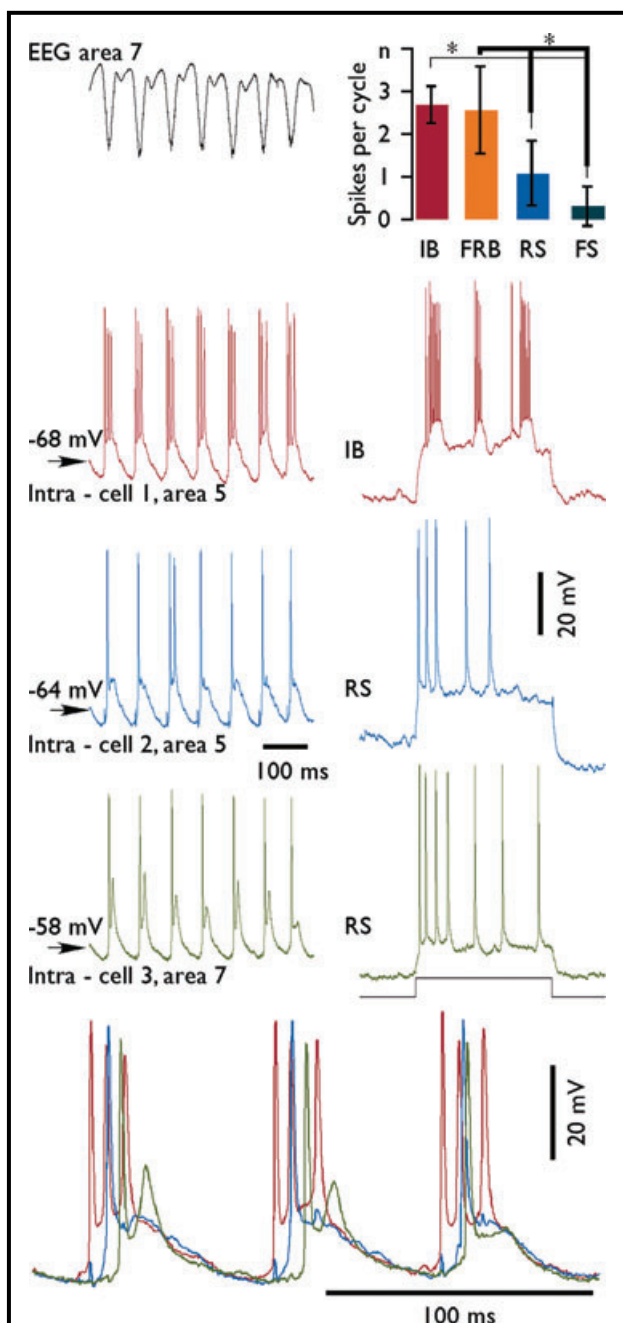


Figure 8.

Discharge patterns of variable electrophysiological types of neurons during fast runs. Left column, field potential and simultaneous triple intracellular recording during a period of fast run. Histogram at upper right corner displays a mean number of spikes generated by neurons of different electrophysiological types during each cycle of paroxysmal fast runs. Electrophysiological identification of neurons from left column is indicated at right. IB, intrinsically-bursting; FRB, fast-rhythmic-bursting; RS, regular spiking neuron; and FS, fast spiking neurons. Statistically significant difference

1990; Gray & McCormick, 1996; Steriade et al., 1998b). The electrophysiological classification of neurons was performed during periods of normal (not paroxysmal) activity. In this set of experiments, we identified 70.6% of neurons as RS, 11.8% as FRB, 11.8% as IB, and the remaining 6 neurons were FS. In each of these neurons, we calculated the mean number of spikes per cycle generated during fast runs (Fig. 8). At least 100 cycles were counted to obtain a mean number of spikes generated by one neuron. Since in many instances the amplitude of spikes was significantly reduced as compared to spikes occurring outside seizures, we counted only spikes that were at least a half of amplitude of a mean spike recorded during normal activities. Some neurons revealed a large variability in the number of spikes per cycle, which could fluctuate from 1 to 6 (Fig. 1, Intra-cell 1). Statistically, we found however that the number of spikes per cycle generated by IB and FRB neurons was significantly higher (Tukey-Kramer HSD test) than the number of spikes generated by other types of neurons (Fig. 8). In addition, IB cells were usually depolarized and fired before any other type of neurons (Fig. 8, bottom panel).

Since, in all the recorded combinations, we observed either repeatable phase shifts or absence of synchrony; our data suggest that fast paroxysmal runs are generated locally. We used a highly simplified network model to demonstrate how extremely variable phase relations can indeed develop between synaptically coupled, oscillating neurons.

Computational model

We have previously shown in a model of isolated cortical PY neuron that increases in $[K^+]_o$ could lead to slow 2- to 3-Hz oscillations and fast runs (Bazhenov et al., 2004). Here we explore phase relations between neurons in different oscillatory states and we show effect of synaptic interaction on the network synchronization.

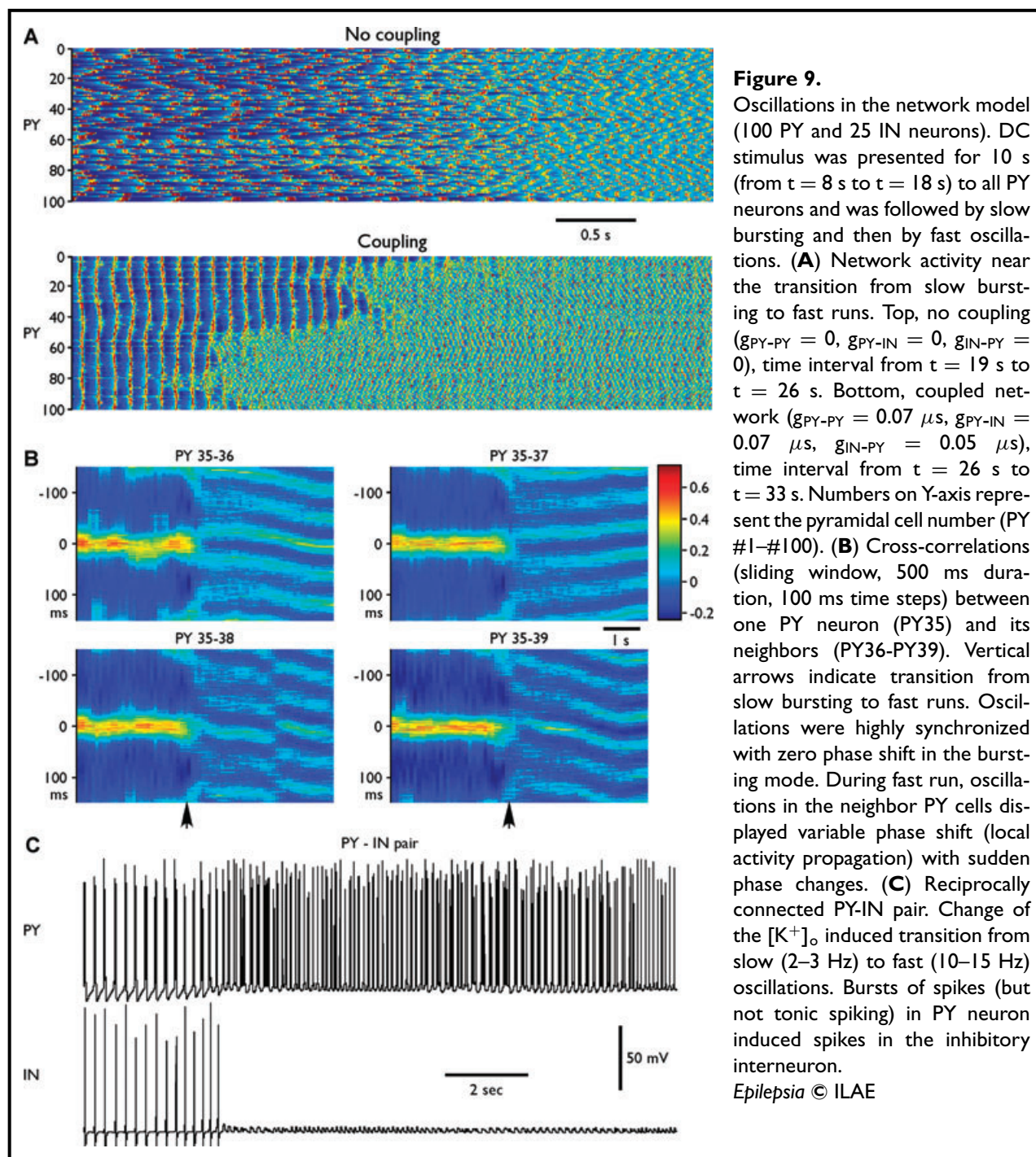
To study synchrony of population oscillations during different oscillatory regimes, we simulated a network model of 100 PY neurons and 25 INs. An external stimulus (DC pulse of 10s) was applied to the network to induce high-frequency spiking in PY cells. Upon DC stimulus termination, all the neurons displayed slow bursting (SW)

←

Continued.

(α , 0.01) is indicated by asterisks. Bottom panel shows the last three cycles of cells presented in the left column at expanded scale. Note that IB cell was depolarized before the two other neurons. Note also the change of delays for depolarization of the green cell compared to the two other cells.

Epilepsia © ILAE



followed by fast spiking (fast runs) (Fig. 9A). We found that: (1) bursting mechanism in this model is essentially mediated by the dynamic interaction of the high threshold calcium and the calcium-activated potassium conductances in PY neurons; (2) progressive decrease of $[K^+]_o$ leads to transition between slow bursting and fast runs; (3) low activity of inhibitory interneurons during fast runs can explain reduced synchrony of these oscillations compare with slow bursting activity.

Because of random variability of the model parameters across neurons and different initial conditions, the neurons in the network model fired independently when synaptic coupling was turned off (Fig. 9A, top). Slow bursting lasted less than 4 s. When excitatory/inhibitory coupling between neurons was included, the slow paroxysmal bursting lasted much longer (~ 10 s) and became synchronized across neurons (Fig. 9A, bottom). Fig. 9B shows cross-correlation between neighbor PY cells in the network; during slow

paroxysmal oscillations these neurons fired with minimal phase delays. A progressive change of $[K^+]_o$ triggered transition from slow to fast oscillations. Similar to in vivo data, neighbor neurons displayed this transition nearly simultaneously; however we found a few large clusters with very different transition times (compare neurons #1–#50 and #51–#100 in Fig. 9A, bottom). Including long-range connections between PY neurons would likely increase the global synchrony of transitions between epochs of slow and fast oscillations. To test this hypothesis, we included random long-range connections between PY neurons and varied probability of long-range coupling p . When $p > 0.02$ – 0.03 , transition from slow bursting to fast runs occurred almost simultaneously with less than 200 ms variability across all neurons in the network (not shown). Thus, synaptic coupling was sufficient to explain synchrony of slow bursting oscillations and fast-slow-fast transitions. Including long-range connections with such low probability did not produce, however, any systematic effect on phase relations between neurons during fast oscillations (see below).

In contrast to the slow bursting mode, during fast runs, the degree of synchrony between neurons (even in close proximity) was significantly reduced even after synaptic coupling was introduced. Typically, neighbor neurons fired with a phase shift, which was consistent for a few cycles of network oscillations thus suggesting local spike propagation. Direction of spike propagation varied from one network site to another. Phase relations between neurons could change from in-phase to out-phase oscillations or vice versa either gradually (see e.g., cross-correlation plot for PY35 and PY36 in Fig. 9B) or suddenly (see e.g., cross-correlation plot for PY35 and PY38 in Fig. 9B).

These modeling results suggest that synaptic coupling between PY neurons and feedback inhibition from active INs may explain synchrony of slow bursting oscillations. Indeed, after synaptic connectivity was introduced in the model, asynchronous firing in all network states (Fig. 9A, top) was replaced by synchronized oscillations in the bursting mode (Fig. 9A, bottom). During fast runs, however, local synaptic excitation, while influenced the phase relations between neighbor neurons, was not sufficient to arrange steady network synchronization. More importantly, the synchronization effect of feedback inhibition was absent during fast runs because of low INs' spiking activity (Fig. 9C). Random long-range connections increased synchrony of transitions between slow bursting and fast runs but could not enhance synchrony of fast oscillations on cycle-to-cycle basis.

DISCUSSION

In this study, we analyzed the spatiotemporal properties of runs of fast EEG spikes recorded during spontaneous

seizures in cats anesthetized with ketamine-xylazine and in computational models. We found that (1) the runs of fast EEG spikes with a frequency of 7–16 Hz often accompanied neocortical seizures; (2) the patterns of synchrony during fast runs were: (i) synchronous, in phase, (ii) synchronous, with phase shift, (iii) patchy, repeated in phase/phase shift transitions, and (iv) nonsynchronous, different frequencies in different recording sites or absence of oscillatory activity in one of the recording sites; the synchronous patterns were most common; (3) the runs of fast spikes appeared as quasi-independent oscillators even in neighboring cortical locations suggesting their focal origin; (4) synchronous fast runs propagated in anterior-posterior direction with a velocity of 2.1–2.2 m/s; and (5) the membrane potential during fast runs was by ~ 9 mV less depolarized as compared to the depolarizing components of SW complexes.

Experimental model of paroxysmal activity

Most of the cats anesthetized with ketamine-xylazine anesthesia, followed by supplementary doses of ketamine-xylazine developed paroxysmal activities consisting of SW discharges at 1–2.5 Hz and runs of fast spikes at 7–16 Hz. These seizures are generated neocortically as (1) they could be obtained in athalamic cats (Steriade & Contreras, 1998), (2) in small neocortical slabs (Timofeev et al., 2000), or (3) in the undercut cortex (Topolnik et al., 2003; Nita et al., 2006; Nita et al., 2007), and (4) most of thalamocortical neurons do not fire during this type of seizures (Steriade & Contreras, 1995; Pinault et al., 1998; Timofeev et al., 1998). The cause of these seizures is unclear. A combination of two major factors could account for the development of those paroxysmal activities.

Slow oscillations

Spontaneously occurring SW complexes at 1–2.5 Hz and fast runs at 7–16 Hz developed without discontinuity from the slow (mainly 0.5–0.9 Hz) cortically generated oscillation (Steriade & Contreras, 1995; Steriade et al., 1998a). Periods of disfacilitation accompanying sleep oscillations activate a large number of intrinsic and synaptic factors leading to the development of seizures (see Timofeev & Steriade, 2004 for the detailed discussion). However, the occurrence of seizures during sleep is far lower than the occurrence of seizures in cats anesthetized with ketamine-xylazine (Steriade et al., 1998a).

Effects of ketamine-xylazine

Ketamine at anesthetic doses blocks *N*-methyl-D-aspartic acid (NMDA)-dependent synaptic events (MacDonald et al., 1991). An activation of NMDA receptors contributes, but is not essential in the generation of paroxysmal discharges (Barkai et al., 1994; Traub et al., 1996). Thus, ketamine should decrease the propensity to the seizure generation. Additional blockage of nicotinic cholinergic receptors by ketamine (Rudolph & Antkowiak, 2004)

would remove their depolarizing action on thalamocortical neurons (McCormick, 1992), low-threshold spiking cortical interneurons (Xiang et al., 1998), and should reduce the efficacy of excitatory synapses formed by thalamocortical neurons on cortical neurons (Gil et al., 1997). However, NMDA blockers at low concentrations could elicit epileptiform burst discharges (Gorji & Speckmann, 2001; Midzyanovskaya et al., 2004).

Xylazine is the agonist of α -2 adrenoreceptors, heavily present in the neocortex (Hedler et al., 1981; Nicholas et al., 1993) that at low doses favors seizures (Joy et al., 1983) and promotes oscillatory behavior of thalamocortical system (Buzsaki et al., 1991). Clonidine, a potent agonist of α -2 receptors inhibited action potential generation of thalamocortical neurons (Funke et al., 1993) and induced changes in the spectral content of the EEG (Sitnikova & van Luijtelaa, 2005). Finally, norepinephrine application, depolarized thalamocortical neurons, suppressed their bursts, leading to tonic firing (McCormick & Prince, 1988). Thus, we suggest that xylazine actions in neocortex largely contribute to the generation of paroxysmal activity induced by ketamine-xylazine anesthesia.

Synaptic interactions and synchronization during seizures

The amplitude of field potentials during SW components of electrographic seizures is higher than the amplitude of slow oscillation (Figs. 2 and 4). This suggests that the focal synchronization during seizures is higher than during the normal brain activities. However, the long-range synchronization during seizures is reduced (Neckelmann et al., 1998; Derchansky et al., 2006). Our modeling data demonstrate that transient seizure-like activity could be obtained in a single cortical neuron, if some extracellular conditions (primarily increased $[K^+]_o$) are present. Therefore, the ligand-dependent synaptic interactions alone do not explain the generation of some form of paroxysmal activities (Johnston & Brown, 1981; Polack & Charpier, 2006). Multiple data support this point of view: (1) Paroxysmal activities are associated with a decreased $[Ca^{2+}]_o$ (Heinemann et al., 1977; Pumain et al., 1983; Amzica et al., 2002), and as a consequence, the effectiveness of synaptic strength decreases, but the intrinsic neuronal excitability increases (Hille, 2001). (2) The use of low or even 0 mM $[Ca^{2+}]_o$ in hippocampal (Leschinger et al., 1993; Pan & Stringer, 1997; Bikson et al., 1999) and cortical (Seigneur J. and Timofeev I., unpublished data) slices in vitro results in the development of epileptiform discharges. (3) The synaptic responsiveness during electrographic seizures in vivo decreases (Steriade & Amzica, 1999; Cisse et al., 2004) and remain reduced after the end of seizures (Nita et al., 2008). (4) The long-range synchronization during seizures, particularly during fast runs, is low or absent (Fig. 4), and finally (5) the neuronal firing dramatically reduces toward the end of the seizure,

while intracellular and field potential activities are ampler as compared to the beginning of the seizure (Bazhenov et al., 2004; Timofeev & Steriade, 2004). In a condition of reduced efficiency of chemical synaptic transmission, the focal neuronal synchronization could be achieved either via electrical coupling between different groups of neurons (Galarreta & Hestrin, 1999; Gibson et al., 1999; Perez Velazquez & Carlen, 2000; Schmitz et al., 2001), glial cells (Amzica et al., 2002), or via ephaptic interactions (Taylor & Dudek, 1982; Taylor & Dudek, 1984a; Taylor & Dudek, 1984b; Grenier et al., 2003a). The mechanisms of electrical coupling have a high efficacy for the short-range synchronization (Galarreta & Hestrin, 2001). During fast runs, the activity of FS interneurons is significantly reduced (Timofeev et al., 2002), and consequently the efficiency of synchronization via electrically coupled interneuronal network (Galarreta & Hestrin, 1999; Gibson et al., 1999; Perez Velazquez & Carlen, 2000) is diminished. The amplitude of field potentials is also reduced (Figs. 1–5) indicating a reduced neuronal synchrony. All five factors discussed above (1–5) are likely contributing to the remarkable loss of synchrony during fast runs.

The onset and the end of fast run occurred almost simultaneously at large cortical distances (Figs. 1 and 2). In Lennox-Gastaut syndrome patients, the runs of fast EEG spikes arise locally (Ohtahara et al., 1995), primarily from frontal lobe (Niedermeyer, 2005a). In cats, the fast runs are also recorded from precruciate gyrus (see Figs. 2 and 4–11 in Timofeev et al., 1998). We demonstrated that fast runs propagate in anterior-posterior direction within suprasylvian gyrus (Fig. 5), likely evolving from frontal cortical areas. The computational model suggests that long-range excitatory connections may account for this synchrony. Another possibility includes the existence of some unknown synchronizing input arriving to the different cortical loci and driving both, the onset, and the end, of fast runs.

Transitions between SW and fast run was also simulated in a cortical column model after fast inhibition was partially blocked (Traub et al., 2005). To simulate SW like patterns, cortical neurons had to be depolarized, reflecting the depolarizing effects of the elevated extracellular K^+ .

Our finding that both IB and FRB neurons fired more spikes during fast runs than the other types of neurons (Fig. 8), imply that bursting neurons could generate the fast runs. The intrinsic tuning of intraburst frequency for FRB neurons is in the range from 20 to 60 Hz (Gray & McCormick, 1996; Steriade et al., 1998b), thus their frequency is much higher than the frequency of paroxysmal fast runs (Fig. 8), and their leading role in the generation of fast runs is doubtful. The intraburst frequency of IB neurons in vivo during normal network activities is around 8 Hz (Nuñez et al., 1993) (see also Fig. 8), which is close to the frequency of fast runs. Seizure related changes in extracellular Ca^{2+} and K^+ concentration (Somjen, 2002) could slightly modulate the intraburst frequency of IB neurons

and thus to cover all range of fast run frequencies. Thus, we suggest that cortical IB neurons play a role of pacemakers during paroxysmal fast runs.

We conclude that the runs of fast EEG spikes, during cortically generated seizures, are generated as quasi-independent oscillators, with very little synaptic communication within cortical network.

ACKNOWLEDGMENTS

We would like to thank P. Giguère for excellent technical assistance. This research was supported by grants from Canadian Institutes of Health Research, Natural Science and Engineering Research Council (I.T.) and NIH-NIDCD (M.B.). I.T. is scholar of Canadian Institutes of Health Research. S.C. is a CIHR fellow.

Conflict of interest: We confirm that we have read the Journal's position on issues involved in ethical publication and affirm that this report is consistent with those guidelines. The authors have no conflicts of interest to declare.

REFERENCES

- Abbott LF, Varela JA, Sen K, Nelson SB. (1997) Synaptic depression and cortical gain control. *Science* 275:220–224.
- Alzheimer C, Schwandt PC, Crill WE. (1993) Modal gating of Na⁺ channels as a mechanism of persistent Na⁺ current in pyramidal neurons from rat and cat sensorimotor cortex. *J Neurosci* 13:660–673.
- Amzica F, Massimini M, Manfridi A. (2002) Spatial buffering during slow and paroxysmal sleep oscillations in cortical networks of glial cells in vivo. *J Neurosci* 22:1042–1053.
- Barkai E, Grossman Y, Gutnick MJ. (1994) Long-term changes in neocortical activity after chemical kindling with systemic pentylentetrazole: an in vitro study. *J Neurophysiol* 72:72–83.
- Bazhenov M, Timofeev I, Steriade M, Sejnowski TJ. (1998) Computational models of thalamocortical augmenting responses. *J Neurosci* 18:6444–6465.
- Bazhenov M, Timofeev I, Steriade M, Sejnowski TJ. (2002) Model of thalamocortical slow-wave sleep oscillations and transitions to activated states. *J Neurosci* 22:8691–8704.
- Bazhenov M, Timofeev I, Steriade M, Sejnowski TJ. (2004) Potassium model for slow (2–3 Hz) in vivo neocortical paroxysmal oscillations. *J Neurophysiol* 92:1116–1132.
- Bikson M, Ghai RS, Baraban SC, Durand DM. (1999) Modulation of burst frequency, duration, and amplitude in the zero-Ca(2+) model of epileptiform activity. *J Neurophysiol* 82:2262–2270.
- Buzsáki G, Kennedy B, Solt VB, Ziegler M. (1991) Noradrenergic control of thalamic oscillation: the role of alpha-2 receptors. *Eur J Neurosci* 3:222–229.
- Chervin RD, Pierce PA, Connors BW. (1988) Periodicity and directionality in the propagation of epileptiform discharges across neocortex. *J Neurophysiol* 60:1695–1713.
- Cisse Y, Crochet S, Timofeev I, Steriade M. (2004) Synaptic responsiveness of neocortical neurons to callosal volleys during paroxysmal depolarizing shifts. *Neuroscience* 124:231–239.
- Connors BW, Gutnick MJ. (1990) Intrinsic firing patterns of diverse neocortical neurons. *Trends Neurosci* 13:99–104.
- Derchansky M, Rokni D, Rick JT, Wennberg R, Bardakjian BL, Zhang L, Yarom Y, Carlen PL. (2006) Bidirectional multisite seizure propagation in the intact isolated hippocampus: the multifocality of the seizure “focus”. *Neurobiol Dis* 23:312–328.
- Destexhe A, Mainen ZF, Sejnowski TJ. (1994) Synthesis of models for excitable membranes, synaptic transmission and neuromodulation using a common kinetic formalism. *J Comput Neurosci* 1:195–230.
- Ferri R, Stam CJ, Lanuzza B, Cosentino FI, Elia M, Musumeci SA, Pennisi G. (2004) Different EEG frequency band synchronization during nocturnal frontal lobe seizures. *Clin Neurophysiol* 115:1202–1211.
- Frohlich F, Bazhenov M. (2006) Coexistence of tonic firing and bursting in cortical neurons. *Phys Rev E Stat Nonlin Soft Matter Phys* 74:031922.
- Frohlich F, Bazhenov M, Timofeev I, Steriade M, Sejnowski TJ. (2006) Slow state transitions of sustained neural oscillations by activity-dependent modulation of intrinsic excitability. *J Neurosci* 26:6153–6162.
- Funke K, Pape HC, Eysel UT. (1993) Noradrenergic modulation of retinogeniculate transmission in the cat. *J Physiol* 463:169–191.
- Galarreta M, Hestrin S. (1998) Frequency-dependent synaptic depression and the balance of excitation and inhibition in the neocortex. *Nat Neurosci* 1:587–594.
- Galarreta M, Hestrin S. (1999) A network of fast-spiking cells in the neocortex connected by electrical synapses. *Nature* 402:72–75.
- Galarreta M, Hestrin S. (2001) Electrical synapses between GABA-releasing interneurons. *Nat Rev Neurosci* 2:425–433.
- Gibson JR, Beierlein M, Connors BW. (1999) Two networks of electrically coupled inhibitory neurons in neocortex. *Nature* 402:75–79.
- Gil Z, Connors BW, Amitai Y. (1997) Differential regulation of neocortical synapses by neuromodulators and activity. *Neuron* 19:679–686.
- Gorji A, Speckmann EJ. (2001) Low concentration of DL-2-amino-5-phosphonovalerate induces epileptiform activity in guinea pig hippocampal slices. *Epilepsia* 42:1228–1230.
- Gray CM, McCormick DA. (1996) Chattering cells: superficial pyramidal neurons contributing to the generation of synchronous oscillations in the visual cortex. *Science* 274:109–113.
- Grenier F, Timofeev I, Crochet S, Steriade M. (2003a) Spontaneous field potentials influence the activity of neocortical neurons during paroxysmal activities in vivo. *Neuroscience* 119:277–291.
- Grenier F, Timofeev I, Steriade M. (2003b) Neocortical very fast oscillations (ripples, 80–200 Hz) during seizures: intracellular correlates. *J Neurophysiol* 89:841–852.
- Halasz P. (1991) Runs of rapid spikes in sleep: a characteristic EEG expression of generalized malignant epileptic encephalopathies. A conceptual review with new pharmacological data. *Epilepsy Res Suppl* 2:49–71.
- Hedler L, Stamm G, Weitzell R, Starke K. (1981) Functional characterization of central alpha-adrenoceptors by yohimbine diastereomers. *Eur J Pharmacol* 70:43–52.
- Heinemann U, Lux HD, Gutnick MJ. (1977) Extracellular free calcium and potassium during paroxysmal activity in the cerebral cortex of the cat. *Exp Brain Res* 27:237–243.
- Hille B. (2001) *Ionic channels of excitable membranes*. Sinauer Associates, Sunderland, MA.
- Hughes SW, Cope DW, Blethyn KL, Crunelli V. (2002) Cellular mechanisms of the slow (<1 Hz) oscillation in thalamocortical neurons in vitro. *Neuron* 33:947–958.
- Johnston D, Brown TH. (1981) Giant synaptic potential hypothesis for epileptiform activity. *Science* 211:294–297.
- Joy RM, Stark LG, Albertson TE. (1983) Dose-dependent proconvulsant and anticonvulsant actions of the alpha 2 adrenergic agonist, xylazine, on kindled seizures in the rat. *Pharmacol Biochem Behav* 19:345–350.
- Kager H, Wadman WJ, Somjen GG. (2000) Simulated seizures and spreading depression in a neuron model incorporating interstitial space and ion concentrations. *J Neurophysiol* 84:495–512.
- Kay AR, Sugimori M, Llinas R. (1998) Kinetic and stochastic properties of a persistent sodium current in mature guinea pig cerebellar Purkinje cells. *J Neurophysiol* 80:1167–1179.
- Kotagal P. (1995) Multifocal independent Spike syndrome: relationship to hypersarrhythmia and the slow spike-wave (Lennox-Gastaut) syndrome. *Clin Electroencephalogr* 26:23–29.
- Leschinger A, Stabel J, Igelmund P, Heinemann U. (1993) Pharmacological and electrographic properties of epileptiform activity induced by elevated K⁺ and lowered Ca²⁺ and Mg²⁺ concentration in rat hippocampal slices. *Exp Brain Res* 96:230–240.
- MacDonald J, Bartlett M, Mody I, Pahapill P, Reynolds J, Salter M, Schneiderman J, Pennefather P. (1991) Actions of ketamine, phencyclidine and MK-801 on NMDA receptor currents in cultured mouse hippocampal neurones. *J Physiol (Lond)* 432:483–508.
- Mainen ZF, Sejnowski TJ. (1996) Influence of dendritic structure on firing pattern in model neocortical neurons. *Nature* 382:363–366.
- Matsumoto H, Ayala GF, Gummit RJ. (1969) Effects of intracellularly injected currents on the PDS and the hyperpolarizing after-potential

- in neurons within an epileptic focus. *Electroencephalogr Clin Neurophysiol* 26:120.
- McCormick DA, Prince DA. (1988) Noradrenergic modulation of firing pattern in guinea pig and cat thalamic neurons, in vitro. *J Neurophysiol* 59:978–996.
- McCormick DA. (1992) Neurotransmitter actions in the thalamus and cerebral cortex and their role in neuromodulation of thalamocortical activity. *Prog Neurobiol* 39:337–388.
- Meeren HK, Pijn JP, Van Luijckelaar EL, Coenen AM, Lopes da Silva FH. (2002) Cortical focus drives widespread corticothalamic networks during spontaneous absence seizures in rats. *J Neurosci* 22:1480–1495.
- Midzyanovskaya IS, Salonin DV, Bosnyakova DY, Kuznetsova GD, van Luijckelaar EL. (2004) The multiple effects of ketamine on electroencephalographic activity and behavior in WAG/Rij rats. *Pharmacol Biochem Behav* 79:83–91.
- Neckelmann D, Amzica F, Steriade M. (1998) Spike-wave complexes and fast components of cortically generated seizures. III. Synchronizing mechanisms. *J Neurophysiol* 80:1480–1494.
- Neckelmann D, Amzica F, Steriade M. (2000) Changes in neuronal conductance during different components of cortically generated spike-wave seizures. *Neuroscience* 96:475–485.
- Nicholas AP, Pieribone V, Hokfelt T. (1993) Distributions of mRNAs for alpha-2 adrenergic receptor subtypes in rat brain: an in situ hybridization study. *J Comp Neurol* 328:575–594.
- Niedermeyer E. (2005a) Abnormal EEG patterns: epileptic and paroxysmal. In Niedermeyer E, Lopes de Silva F (Eds) *Electroencephalography: basic principles, clinical applications, and related fields*. Williams & Wilkins, Baltimore, pp. 255–280.
- Niedermeyer E. (2005b) Epileptic seizure disorders. In Niedermeyer E, Lopes de Silva F (Eds) *Electroencephalography: basic principles, clinical applications, and related fields*. Williams & Wilkins, Baltimore, pp. 505–620.
- Nita D, Cissé Y, Timofeev I, Steriade M. (2006) Increased propensity to seizures after chronic cortical deafferentation in vivo. *J Neurophysiol* 95:902–913.
- Nita DA, Cisse Y, Timofeev I, Steriade M. (2007) Waking-sleep modulation of paroxysmal activities induced by partial cortical deafferentation. *Cereb Cortex* 17:272–283.
- Nita DA, Cisse Y, Timofeev I. (2008) EPSP depression following neocortical seizures in cat. *Epilepsia* 49:705–709.
- Núñez A, Amzica F, Steriade M. (1993) Electrophysiology of cat association cortical cells in vitro: intrinsic properties and synaptic responses. *J Neurophysiol* 70:418–430.
- Ohtahara S, Ohtsuka Y, Kobayashi K. (1995) Lennox-Gastaut syndrome: a new vista. *Psychiatry Clin Neurosci* 49:S179–S183.
- Pan E, Stringer JL. (1997) Role of potassium and calcium in the generation of cellular bursts in the dentate gyrus. *J Neurophysiol* 77:2293–2299.
- Perez Velazquez JL, Carlen PL. (2000) Gap junctions, synchrony and seizures. *Trends Neurosci* 23:68–74.
- Pinault D, Leresche N, Charpier S, Deniau JM, Marescaux C, Vergnes M, Crunelli V. (1998) Intracellular recordings in thalamic neurones during spontaneous spike and wave discharges in rats with absence epilepsy. *J Physiol* 509:449–456.
- Polack P-O, Charpier S. (2006) Intracellular activity of cortical and thalamic neurones during high-voltage rhythmic spike discharge in Long-Evans rats in vivo. *J Physiol* 571:461–476.
- Pumain R, Kurcewicz I, Louvel J. (1983) Fast extracellular calcium transients: involvement in epileptic processes. *Science* 222:177–179.
- Rudolph U, Antkowiak B. (2004) Molecular and neuronal substrates for general anesthetics. *Nat Rev Neurosci* 5:709–720.
- Rulkov NF, Timofeev I, Bazhenov M. (2004) Oscillations in large-scale cortical networks: map-based model. *J Comput Neurosci* 17:203–223.
- Schmitz D, Schuchmann S, Fisahn A, Draguhn A, Buhl EH, Petrasch-Parwez E, Dermietzel R, Heinemann U, Traub RD. (2001) Axo-axonal coupling a novel mechanism for ultrafast neuronal communication. *Neuron* 31:831–840.
- Sitnikova E, van Luijckelaar G. (2005) Reduction of adrenergic neurotransmission with clonidine aggravates spike-wave seizures and alters activity in the cortex and the thalamus in WAG/Rij rats. *Brain Res Bull* 64:533–540.
- Somjen GG. (2002) Ion regulation in the brain: implications for pathophysiology. *Neuroscientist* 8:254–267.
- Steriade M, Contreras D. (1995) Relations between cortical and thalamic cellular events during transition from sleep patterns to paroxysmal activity. *J Neurosci* 15:623–642.
- Steriade M, Contreras D. (1998) Spike-wave complexes and fast components of cortically generated seizures. I. Role of neocortex and thalamus. *J Neurophysiol* 80:1439–1455.
- Steriade M, Amzica F, Neckelmann D, Timofeev I. (1998a) Spike-wave complexes and fast components of cortically generated seizures. II. Extra- and intracellular patterns. *J Neurophysiol* 80:1456–1479.
- Steriade M, Timofeev I, Dürmüller N, Grenier F. (1998b) Dynamic properties of corticothalamic neurons and local cortical interneurons generating fast rhythmic (30–40 Hz) spike bursts. *J Neurophysiol* 79:483–490.
- Steriade M, Amzica F. (1999) Intracellular study of excitability in the seizure-prone neocortex in vivo. *J Neurophysiol* 82:3108–3122.
- Steriade M, Timofeev I. (2001) Corticothalamic operations through prevalent inhibition of thalamocortical neurons. *Thalamus Relat Syst* 1:225–236.
- Taylor CP, Dudek FE. (1982) Synchronous neural afterdischarges in rat hippocampal slices without active chemical synapses. *Science* 218:810–812.
- Taylor CP, Dudek FE. (1984a) Excitation of hippocampal pyramidal cells by an electrical field effect. *J Neurophysiol* 52:126–142.
- Taylor CP, Dudek FE. (1984b) Synchronization without active chemical synapses during hippocampal afterdischarges. *J Neurophysiol* 52:143–155.
- Timofeev I, Grenier F, Steriade M. (1998) Spike-wave complexes and fast components of cortically generated seizures. IV. Paroxysmal fast runs in cortical and thalamic neurons. *J Neurophysiol* 80:1495–1513.
- Timofeev I, Grenier F, Bazhenov M, Sejnowski TJ, Steriade M. (2000) Origin of slow cortical oscillations in deafferented cortical slabs. *Cereb Cortex* 10:1185–1199.
- Timofeev I, Grenier F, Steriade M. (2002) The role of chloride-dependent inhibition and the activity of fast-spiking neurons during cortical spike-wave seizures. *Neuroscience* 114:1115–1132.
- Timofeev I, Steriade M. (2004) Neocortical seizures: initiation, development and cessation. *Neuroscience* 123:299–336.
- Topolnik L, Steriade M, Timofeev I. (2003) Partial cortical deafferentation promotes development of paroxysmal activity. *Cereb Cortex* 13:883–893.
- Traub RD, Borck C, Colling SB, Jefferys JG. (1996) On the structure of ictal events in vitro. *Epilepsia* 37:879–891.
- Traub RD, Contreras D, Cunningham MO, Murray H, LeBeau FEN, Roopun A, Bibbig A, Wilentz WB, Hügley MJ, Whittington MA. (2005) Single-column thalamocortical network model exhibiting gamma oscillations, sleep spindles, and epileptogenic bursts. *J Neurophysiol* 93:2194–2232.
- Tsodyks MV, Markram H. (1997) The neural code between neocortical pyramidal neurons depends on neurotransmitter release probability. *Proc Natl Acad Sci U S A* 94:719–723.
- Xiang Z, Huguenard JR, Prince DA. (1998) Cholinergic switching within neocortical inhibitory networks. *Science* 281:985–988.